IEEE Access
Multidisciplinary | Rapid Review | Open Access Journal

Received March 15, 2021, accepted April 6, 2021, date of publication April 12, 2021, date of current version April 20, 2021.

Digital Object Identifier 10.1109/ACCESS.2021.3072452

Real-Time Multibody Model-Based Heads-Up Display Unit of a Tractor

SURAJ JAISWAL[1], RAFAEL ÅMAN[2], JUSSI SOPANEN[1], (Member, IEEE), AND AKI MIKKOLA[1]

[1]Department of Mechanical Engineering, Lappeenranta University of Technology, 53850 Lappeenranta, Finland
[2]Valtra Inc., 44200 Suolahti, Finland

Corresponding author: Suraj Jaiswal (suraj.jaiswal@lut.fi)

This work was supported in part by the Business Finland (Project: Service Business from Physics Based Digital Twins—DigiBuzz), and in part by the Academy of Finland under Grant 316106.

ABSTRACT The concept of heads-up display can be used to provide augmented information onto the windshield of a tractor. The objective of this paper is to introduce a detailed real-time multibody model that is used in the design of a novel heads-up display unit of a tractor. To this end, a tractor is described using a multibody dynamics approach. A heads-up display unit is designed using a series of tasks that are associated with sets of logical conditions and instructions. These conditions and instructions, in turn, determine/design the analog and digital gauges. The gauges are linked with the virtual sensors installed at a number of locations on the tractor. In this study, the heads-up display unit includes elements, such as tachometer, speedometer, roll inclinometer, gear indicator, fuel gauge, and bucket height, tilt, and weight indicators. The effectiveness of the heads-up display unit is determined based on a goal of moving a certain amount of sand from one place to another. The results demonstrate the utility of the heads-up display unit.

INDEX TERMS Multibody dynamics, heads-up display, real-time simulation, tractor model, physics-based model.

I. INTRODUCTION

In the last decade, driving aids such as heads-up displays (HUDs) have gained considerable popularity from vehicle manufacturers [1]–[5]. HUDs present augmented machine data usually on the windshield such that drivers do not have to look away from their conventional viewpoints. In practice, a rapid prototype-based development of such HUDs may be expensive or cumbersome [6]. However, a HUD unit can be modeled from a detailed physics-based model of a vehicle using virtual sensing, that is, by incorporating detailed vehicle dynamics. It can allow vehicle manufacturers to test HUDs for their vehicles using computer simulations even before a physical prototype implementation. Additionally, it can be utilized in user training, research, and other product processes.

A. RELATED WORK–LITERATURE REVIEW

It is well established in the literature that classical dashboard displays or head-down displays (HDDs) cause distractions [7] that can be alleviated by HUDs [8]–[10]. They serve a better alternative to provide machine data and increase road safety [11], [12]. It is demonstrated in [10], [13] that drivers can have faster focal re-accommodation time with HUDs and can maintain a consistent speed control. Moreover, HUDs can help novice drivers to get familiarized with control systems [10] and to enhance the surrounding awareness of a vehicle en-route [14]. The studies on HUDs in general are mainly focused towards the field of cognitive science such as human behavior or user experience [15]. On the contrary, the scope of this study is limited to the development of tool sets to model HUD units.

The literature offers several studies regarding HUD modeling and their evaluation on driving simulators. For example, a HUD-based warning system was proposed in [16] to evaluate drivers' rear-end crash avoidance behavior when a leading vehicle makes an emergency stop under foggy conditions. Similarly, HUD-based speed assistance was developed in [17] to provide speed-guided messages through the entire course of curve driving. The HUDs in [16], [17] were tested on the National Advanced Driving Simulator (NADS MiniSim) [18]. Even though the NADS MiniSim is based on multibody dynamics (usage of which leads to realistic simulations), however, the studies in [16] and [17] overlooked

The associate editor coordinating the review of this manuscript and approving it for publication was Lei Wei.

the connection between HUD modeling and detailed vehicle models. Furthermore, a full-windshield HUD model was proposed in [14] to improve drivers' spatial awareness and response time during navigation under low visibility. This HUD model was extended in [19] by incorporating a gesture recognition system [20] to improve human responses during a potential collision and slow down the plethora of incoming information. The respective multimodal and augmented reality (AR) versions of this HUD model [19] was developed in [21] and [22] to alleviate the cognitive load caused by the existing attention seeking HDDs. The HUD models in [14], [19], [21], [22] were based on a minimalist visual display of real objects, however, these studies ignored the description of vehicle models used in the respective simulators.

Many studies in the literature are focused on examining various HUD models in real vehicles. For example, HUD-based advisory speed assistance was developed in [23] using a learning-based approach to compensate drivers generated speed tracking errors in real-time. Testing was carried out in the Unity game engine and a real vehicle, where simulation results deviated from reality. Similarly, navigation-based AR-HUDs were studied in [24], [25] to examine drivers' performance in simulation [25] and real-world environments. In [24], simulations were carried out in the Unreal Engine and on-road testing was carried out on a HUD-equipped real vehicle, whereas AR-HUD interfaces were developed in Unity. Simulation results even here deviated from real-world tests. Furthermore, fixed and animated designs of AR-HUDs were examined in [26] to evaluate drivers' performance and visual behavior in goal-directed and stimulus-driven tasks. AR graphics were rendered in C++ and QT5 environment and testing was performed on a real vehicle that was equipped with a projection-based volumetric HUD. In all the studies above [23], [24], [26], either tests were performed with real vehicles or simulation outcomes deviated from reality, and the lack of detailed physics-based vehicle dynamics in simulation models can be a possible cause. Studies are even directed towards eliminating the display error of HUD models, such as in [27] and [28]. However, these studies [27], [28] used either a stationary vehicle or utilized real-world driving images and ignored vehicle dynamics.

Multibody dynamics can describe detailed physics-based models of complex systems such like a tractor [29], [30]. This approach allows one to describe a large number of bodies, hydraulic actuators, contact models, and tire models. In the literature, a number of multibody dynamics approaches have been used to describe various heavy-duty vehicles. For example, an excavator was described in [31], [32] and [33], a quadtrac in [34], a tree harvester in [35], and a tractor in [36]. Solution of multibody equations of motion can be synchronized to real-time as shown in [32], [35] and [36]. Moreover, virtual sensors can be built using a multibody model such as in [37], [38].

Despite the previous research efforts as explained above, the limitations of the exiting literature are in two manifolds. First, even though the studies on HUDs provide detailed explanations about HUD modeling, however, its connection with the detailed physics-based model of a vehicle has been overlooked. Second, even though the literature on multibody dynamics can accurately describe real-time capable vehicle dynamics, however, the use of such vehicle models in designing HUD has been neglected. Therefore, this study claims to cover this research gap by introducing HUD modeling based on a detailed physics-based vehicle model.

B. OBJECTIVE AND RESEARCH QUESTIONS

The objective of this paper is to introduce a detailed real-time multibody model-based novel heads-up display unit of a tractor. To this end, a tractor is described using a semi-recursive multibody formulation [39] and the hydraulic actuators are described using the lumped fluid theory [40]. In this study, the contact is described using the object-oriented bounding box and penalty methods [41], [42], and the tires are described using the lumped LuGre model [43], [44]. A heads-up display unit is designed onto the windshield of the tractor using a series of tasks that are associated with sets of logical conditions and instructions. The conditions and instructions determine/design the analog and digital gauges, which, in turn, are linked with the virtual sensors installed at a number of locations on the tractor. The advantage of using a multibody dynamics approach is that virtual sensors can be described using the multibody model of the tractor. This enables a flexible approach to design a HUD unit and collect user experience on it before its implementation into a real tractor. In this study, the HUD unit includes elements that are possible to implement into a physical tractor, such as tachometer, speedometer, roll inclinometer, gear indicator, fuel gauge, and bucket height, tilt, and weight indicators. Examples of moving a certain amount of sand from one place to another are demonstrated. Therefore, this study aims to solve the following research questions: (a) How can a HUD model be build using a detailed physics-based model of a vehicle, such as a tractor?; (b) How can such a HUD unit assist drivers to perform a certain work?; and (c) How robust and modular is this HUD modeling approach to contribute to the state-of-the-art?

This paper contains five sections. The structure for the rest of the paper is organized such that Sect. II describes the multibody modeling method. Section III describes the modeling procedure for a heads-up display unit based on a detailed real-time multibody model of a tractor. Section IV provides simulation results and discussion of various tests conducted. A conclusion is provided in Sect. V.

II. MULTIBODY DYNAMICS

The equations of motion for a constrained mechanical system can be described using a multibody dynamics approach. This approach allows one to describe systems of other physical nature, such as hydraulic actuators. In this study, the multibody system is described using a semi-recursive formulation based on a velocity transformation [39] because it allows one to describe vehicles for real-time applications [32], [36].

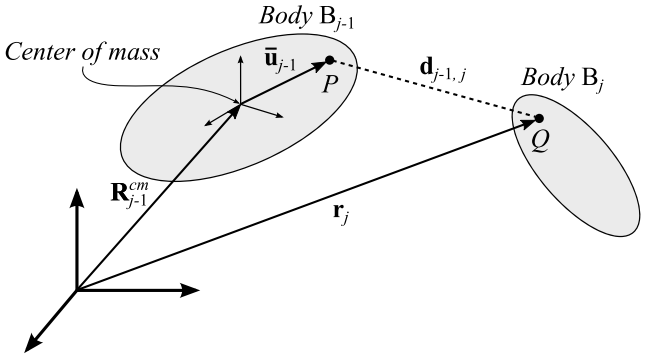

FIGURE 1. Illustration of a multibody system.

The hydraulic actuators are described using the lumped fluid theory [40]. In this study, the contacts are described using the object-oriented bounding box method [41] and penalty method [42]. Furthermore, the tires are described using the lumped LuGre tire model [43], [44].

A. SEMI-RECURSIVE MULTIBODY FORMULATION

In the semi-recursive formulation, the equations of motion are expressed in the relative joint coordinates by using a velocity transformation matrix [39]. Consider an open-loop system with N_b bodies, where the adjacent rigid bodies B_{j-1} and B_j are connected by a joint as shown in Fig. 1. Points P and Q are, respectively, the locations of joints on bodies B_{j-1} and B_j, and $\mathbf{d}_{j-1,j}$ is the relative joint displacement vector between them.

The position, $\mathbf{r}_j$, and the velocity, $\dot{\mathbf{r}}_j$, of point Q with respect to the inertial reference frame can be, respectively, written as

$$\mathbf{r}_j = \mathbf{R}^{cm}_{j-1} + \mathbf{A}_{j-1}\bar{\mathbf{u}}_{j-1} + \mathbf{d}_{j-1,j}, \tag{1}$$

$$\dot{\mathbf{r}}_j = \dot{\mathbf{R}}^{cm}_{j-1} + \widetilde{\boldsymbol{\omega}}_{j-1}\mathbf{A}_{j-1}\bar{\mathbf{u}}_{j-1} + \dot{\mathbf{d}}_{j-1,j}, \tag{2}$$

where $\mathbf{R}^{cm}_{j-1}$ is the position of the origin of the body reference frame of body B_{j-1} with respect to the inertial reference frame and $\dot{\mathbf{R}}^{cm}_{j-1}$ is its time derivative, $\mathbf{A}_{j-1}$ and $\widetilde{\boldsymbol{\omega}}_{j-1}$ are, respectively, the rotation matrix and skew-symmetric matrix of the angular velocity $\boldsymbol{\omega}_{j-1}$ of body B_{j-1}, $\bar{\mathbf{u}}_{j-1}$ is the position vector of point P in the body reference frame of body B_{j-1}, and $\dot{\mathbf{d}}_{j-1,j}$ is the time derivative of $\mathbf{d}_{j-1,j}$. The body reference frames are located at the center of mass of the bodies. The rotation matrix, $\mathbf{A}_j$, and angular velocity, $\boldsymbol{\omega}_j$, of body B_j can be, respectively, written as

$$\mathbf{A}_j = \mathbf{A}_{j-1}\mathbf{A}_{j-1,j}, \tag{3}$$

$$\boldsymbol{\omega}_j = \boldsymbol{\omega}_{j-1} + \boldsymbol{\omega}_{j-1,j}, \tag{4}$$

where $\mathbf{A}_{j-1,j}$ and $\boldsymbol{\omega}_{j-1,j}$ are, respectively, the relative rotation matrix and relative angular velocity between the two bodies B_{j-1} and B_j. In this study, Euler parameters are used to describe a body's rotation.

By using the principle of virtual work, the virtual power of the forces acting on a multibody system can be expressed as [39]

$$\delta\dot{\mathbf{q}}^{\mathrm{T}}\left(\mathbf{M}\ddot{\mathbf{q}} + \mathbf{C} - \mathbf{Q}\right) = \mathbf{0}, \tag{5}$$

where $\delta\dot{\mathbf{q}}$ is the virtual velocity vector, $\mathbf{M}$ is the mass matrix of the system, $\ddot{\mathbf{q}}$ is the absolute acceleration vector, $\mathbf{C}$ is the quadratic velocity vector, and $\mathbf{Q}$ is the vector of external forces and torques acting on the system. Note that $\ddot{\mathbf{q}} = [\ddot{\mathbf{q}}_1^{\mathrm{T}}\ddot{\mathbf{q}}_2^{\mathrm{T}}\ldots\ddot{\mathbf{q}}_{N_b}^{\mathrm{T}}]^{\mathrm{T}}$, $\mathbf{C} = [\mathbf{C}_1^{\mathrm{T}}\mathbf{C}_2^{\mathrm{T}}\ldots\mathbf{C}_{N_b}^{\mathrm{T}}]^{\mathrm{T}}$, and $\mathbf{Q} = [\mathbf{Q}_1^{\mathrm{T}}\mathbf{Q}_2^{\mathrm{T}}\ldots\mathbf{Q}_{N_b}^{\mathrm{T}}]^{\mathrm{T}}$. Furthermore, the virtual velocities $\delta\dot{\mathbf{q}}$ are assumed to be kinematically admissible, implying that they satisfy the equations of kinematic constraints. A velocity transformation matrix, $\mathbf{R}$, is introduced to transform the absolute coordinates into the relative joint coordinates as

$$\dot{\mathbf{q}} = \mathbf{R}\dot{\mathbf{z}}, \tag{6}$$

$$\ddot{\mathbf{q}} = \mathbf{R}\ddot{\mathbf{z}} + \dot{\mathbf{R}}\dot{\mathbf{z}}, \tag{7}$$

where $\dot{\mathbf{q}}$ is the absolute velocity vector, $\dot{\mathbf{z}}$ is the relative joint velocity vector, $\ddot{\mathbf{z}}$ is the relative joint acceleration vector, and $\dot{\mathbf{R}}$ is the time derivative of $\mathbf{R}$. For scleronomic constraints, the kinematically admissible virtual velocities can be written as

$$\delta\dot{\mathbf{q}} = \mathbf{R}\delta\dot{\mathbf{z}}. \tag{8}$$

By substituting Eqs. (7) and (8) into Eq. (5), the equations of motion for an open-loop system can be written as

$$\mathbf{R}^{\mathrm{T}}\mathbf{M}\mathbf{R}\ddot{\mathbf{z}} = \mathbf{R}^{\mathrm{T}}(\mathbf{Q} - \mathbf{C}) - \mathbf{R}^{\mathrm{T}}\mathbf{M}\dot{\mathbf{R}}\dot{\mathbf{z}}. \tag{9}$$

Equation (9) presents N_f numbers of ordinary differential equations of motion that are expressed in relative joint coordinates. The computational efficiency of this formulation is dependent on the computation of the velocity transformation matrix, $\mathbf{R}$, which in this study is obtained using an element by element technique as in [30].

For a closed-loop system, a cut-joint is introduced in each kinematic loop to make it an open-loop system, as shown above. The loop-closure constraint equations are incorporated in the equations of motion by using the penalty method [45] as explained in [39].

B. HYDRAULIC ACTUATORS

In this study, the lumped fluid theory is used to compute the pressures in a hydraulic circuit [40]. In this approach, a hydraulic circuit is divided into separate volumes where the hydraulic pressures are assumed to be equally distributed. Therefore, the effects of acoustic waves are assumed insignificant in this study. The hydraulic pressure, p_s, within a hydraulic control volume, V_s, can be computed as

$$\dot{p}_s = \frac{B_{e_s}}{V_s}\sum_{k=1}^{n_f} Q_{sk}, \tag{10}$$

where B_{e_s} is the effective bulk modulus, Q_{sk} is the sum of volume flow rates in and out of a volume V_s, and n_f is the total number of such volume flow rates.

In this study, the directional control valves are described by using a semi-empirical modeling method [46]. The volume

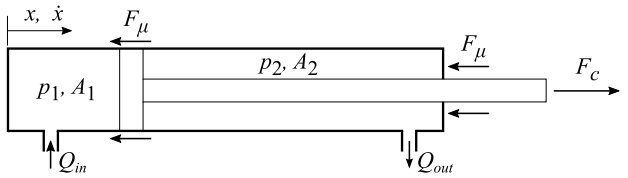

FIGURE 2. A hydraulic actuator.

flow rate, Q, through a directional control valve can be written as

$$Q = C_v U \,\mathrm{sgn}(\Delta p)\sqrt{|\,\Delta p\,|}, \tag{11}$$

where Δp is the pressure difference across the directional control valve, C_v is the semi-empirical flow rate constant of the valve that can be obtained from the manufacturer catalogue, and U is the relative spool position that can be described as

$$\dot{U} = \frac{U_{ref} - U}{\tau}, \tag{12}$$

where τ is the time constant and U_{ref} is the reference voltage signal for the reference spool position.

Furthermore, the force, F_c, produced by a hydraulic actuator, as shown in Fig. 2, can be written as [47]

$$F_c = p_1 A_1 - p_2 A_2 - F_\mu, \tag{13}$$

where A_1 and A_2 are, respectively, the areas of the piston and piston-rod sides of the actuator, p_1 and p_2 are, respectively, the chamber pressures on the piston and piston-rod sides, and F_μ is the total seal friction [48].

C. CONTACT MODELING

The contact model in this study is described in two steps: collision detection and collision response [49]. Collision detection is determined using the object-oriented bounding box method [41], which utilizes minimum rectangular solids as shown in Fig. 3 to circumscribe the bodies along their axes directions. In Fig. 3, the condition that two boxes E and F do not overlap can be written as

$$\mathbf{T} \cdot \mathbf{L}_i > d_{Ei} + d_{Fi}, \tag{14}$$

where

$$d_{Ei} = e_1\mathbf{E}_1 \cdot \mathbf{L}_i + e_2\mathbf{E}_2 \cdot \mathbf{L}_i, \tag{15}$$
$$d_{Fi} = f_1\mathbf{F}_1 \cdot \mathbf{L}_i + f_2\mathbf{F}_2 \cdot \mathbf{L}_i, \tag{16}$$

where $\mathbf{T}$ is the position vector between the center of the boxes, $\mathbf{L}_i$ is a separating axis in a normalized direction, e_1 and e_2, and f_1 and f_2 are, respectively, the dimensions of boxes E and F, and $\mathbf{E}_1$ and $\mathbf{E}_2$, and $\mathbf{F}_1$ and $\mathbf{F}_2$ are, respectively, the normalized axes of boxes E and F. In three dimensions, the condition shown in Eq. (14) such that the boxes do not overlap needs to hold true for all the 15 potential separating axes, implying that $i = 1 : 15$.

The collision response is determined using the penalty method [42]. Assuming a single collision point model,

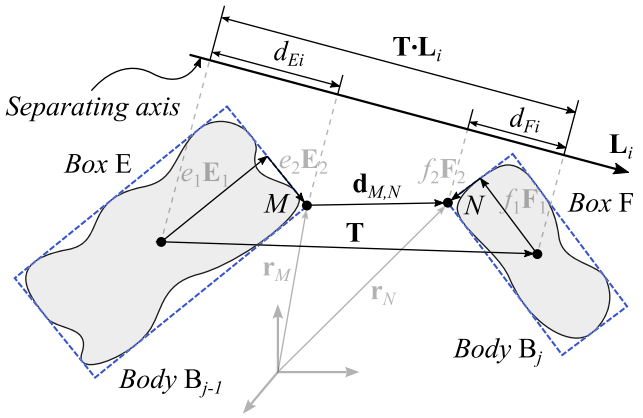

FIGURE 3. Illustration of contact modeling.

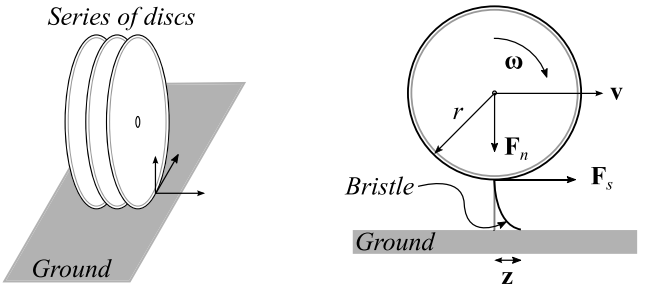

FIGURE 4. Illustration of the lumped LuGre tire model.

the normal contact force, $\mathbf{F}_n$, at the collision point can be written as

$$\mathbf{F}_n = -\left(K\left|\mathbf{d}_{M,N}\right| + C\left|\dot{\mathbf{d}}_{M,N}\right|\right)\mathbf{n}, \tag{17}$$

where

$$\left|\mathbf{d}_{M,N}\right| = (\mathbf{r}_N - \mathbf{r}_M)\cdot\mathbf{n}, \tag{18}$$
$$\left|\dot{\mathbf{d}}_{M,N}\right| = (\dot{\mathbf{r}}_N - \dot{\mathbf{r}}_M)\cdot\mathbf{n}, \tag{19}$$

where K is the coefficient of elasticity, C is the damping factor, $\mathbf{r}_M$ and $\mathbf{r}_N$, and $\dot{\mathbf{r}}_M$ and $\dot{\mathbf{r}}_N$ are, respectively, the positions and velocities of collision points M and N in the inertial reference frame, and $\mathbf{n}$ is the vector along the collision normal such that $\mathbf{n} = \frac{(\mathbf{r}_N - \mathbf{r}_M)}{|(\mathbf{r}_N - \mathbf{r}_M)|}$.

D. TIRE MODELING

In this study, the lumped LuGre tire model [43], [44] is used to model a tire as shown in Fig. 4. Furthermore, a tire is described as a series of discs as shown in Fig. 4 (on the left), where the typical forces involved are the longitudinal, vertical, and lateral forces. The lumped LuGre tire model is an extension of the Dahl model [50] and includes the Stribeck and stiction effects. Based on the lumped LuGre tire model, the friction force, $\mathbf{F}_s$, at the contact between a tire and a ground can be written as [43]

$$\mathbf{F}_s = (\sigma_0\mathbf{z} + \sigma_1\dot{\mathbf{z}} + \sigma_2\mathbf{v}_r)\,\mathbf{F}_n, \tag{20}$$

where

$$\dot{\mathbf{z}} = \mathbf{v}_r - \frac{\sigma_0\mathbf{v}_r}{g(\mathbf{v}_r)}\mathbf{z}, \tag{21}$$

$$g(\mathbf{v}_r) = \mu_c + (\mu_s - \mu_c)\,e^{-\left(\frac{|\mathbf{v}_r|}{v_s}\right)^{\frac{1}{2}}}, \tag{22}$$

where $\mathbf{z}$ is the average bristle deflection (an internal state variable), σ_0 and σ_1 are, respectively, the longitudinal lumped stiffness and damping of the rubber, σ_2 is the coefficient of viscous friction, $\mathbf{v}_r$ is the relative tangential velocity between the tire and ground, $\mathbf{F}_n$ is the normal force, μ_c and μ_s are, respectively, the normalized Coulomb and static frictions such that $\mu_c \leq \mu_s \in [0, 1]$, and $\mathbf{v}_s$ is the Stribeck velocity. Note that $|\mathbf{v}_r| = r\,|\boldsymbol{\omega}| - |\mathbf{v}|$, where r, $\boldsymbol{\omega}$, and $\mathbf{v}$ are respectively, the radius, angular velocity, and linear velocity of the tire.

III. MULTIBODY MODEL-BASED HEADS-UP DISPLAY UNIT

Using the multibody dynamics explained in Sect. II, a detailed physics-based tractor can be modeled as in this study. It should be noted that the focus of this study is to introduce a HUD unit of a tractor, which is based on a real-time multibody model. Accordingly, a semi-recursive multibody formulation that is based on a velocity transformation [39] is utilized to demonstrate a wide capability of real-time multibody models. However, the scope of this study is not limited to a single multibody formulation only. Other multibody formulations that provide real-time capabilities are also applicable, such as index-3 augmented Lagrangian semi-recursive formulation [51], [52] and double-step semi-recursive formulation [53]–[55]. It is also important to note that the used multibody formulation can be applied to wide variety of HUD studies.

A. MULTIBODY MODEL OF A TRACTOR

As a case example, a tractor is modeled using the semi-recursive multibody formulation explained in Sect. II-A. The bodies and joints used in the tractor model are shown in Fig. 5a. Modeling the mechanical system of the tractor can be divided into two parts: modeling the tractor vehicle and modeling the front-loader. The components of the tractor vehicle consist of the cabin, frame, front axle, tie rod, pivot left, and pivot right. The tie rod is used to model the steering mechanism. The components of the front-loader consist of links 1 to 6 and the bucket. The lifting of link-3 and the tilting of link-6 is controlled using hydraulic actuators as explained in Sect. II-B. The power transmission system used in the modeling of the tractor is shown in Fig. 5b.

Overall, the tractor model consists of 13 bodies and 15 joints, and a total of 28 joint coordinates. The structure consists of both open and close kinematic loops, therefore, for the closed-loop links, three cut-joints as shown in Fig. 5 and 15 loop-closure constraints are introduced. The model has nine degrees of freedom (DOFs), where six DOFs correspond to the translational and rotational axes of the tractor, one DOF corresponds to the steering mechanism, and two DOFs correspond to the lifting and tilting mechanism of the front-loader.

Furthermore, four hydraulic actuators are modeled using the lumped fluid theory, explained in Sect. II-B, to lift and tilt the front loader as shown in Fig. 5. Here, the internal dynamics of the hydraulic system are computed, and the resultant forces are combined with the force vector of the multibody equations of motion as in [56]. It should be noted that leakage is neglected in the hydraulic system model. In addition, a deformable ground (sand field) is modeled as in [36], which allows the bucket to fill physically and visually accurate sand particles. The interaction between the force points, defined on the collision geometry of the bucket, and sand field generates sand particles. Tires are modeled using the lumped LuGre tire model as explained in Sect. II-D.

B. HEADS-UP DISPLAY UNIT OF A TRACTOR

Operating a tractor can be cumbersome because its human–machine interface is not simple and requires years of on-the-job training and education. Other than driving, the primary aim in a tractor is to interact with its environment, and the present human–machine interface offers inadequate information about its surroundings and poor work visibility. HUDs can alleviate this problem by presenting more visual clues about the sensor systems of the vehicle in the field-of-view of drivers, thus, providing a quantitative picture of the surroundings [57]. However, the positioning and differences in the perception of HUD images can cause undue mental and physical workloads that can reduce the productivity of drivers through impaired concentration and fatigue [58]. Therefore, care should be taken in general to follow adequate image displaying method [58] that can reduce the cognitive load of drivers, increase their efficiency, and decrease energy costs. Furthermore, presenting machine data on a small area of a windshield impose limitations on the amount of machine information being displayed [59]. It can cause information overload, visual clutter, cognitive capture, and distorted perception of surrounding objects, which can adversely affect the driving performance [60]–[62]. Therefore, understanding drivers' information need can be crucial [5], however, it is not covered within the scope of this study.

A tractor with a front-loader can interact with its environment in several ways [63]. For example, it can load and transfer materials from one place to another, or it can collide with the objects of the environment. The loading and transferring of material are a common task for a tractor, and in such a situation, the driver has a limited information about the bucket position, bucket angle, and weight in the bucket. Therefore, a HUD unit with an effective symbology design can provide these data to improve drivers' performance and reduce their workload. Accordingly, the scope of this work covers both analog and digital gauges in the HUD unit. It should be noted that care is taken to model the design, complexity, image quality, and perceptibility of the HUD unit in an acceptable manner, keeping in mind the cognitive and sensory abilities of drivers [15].

In this study, a simple goal is demonstrated where a certain amount of sand needs to be picked from a sand pile and then dumped onto another place on the ground. In the process, a HUD unit is available to assist the driver,

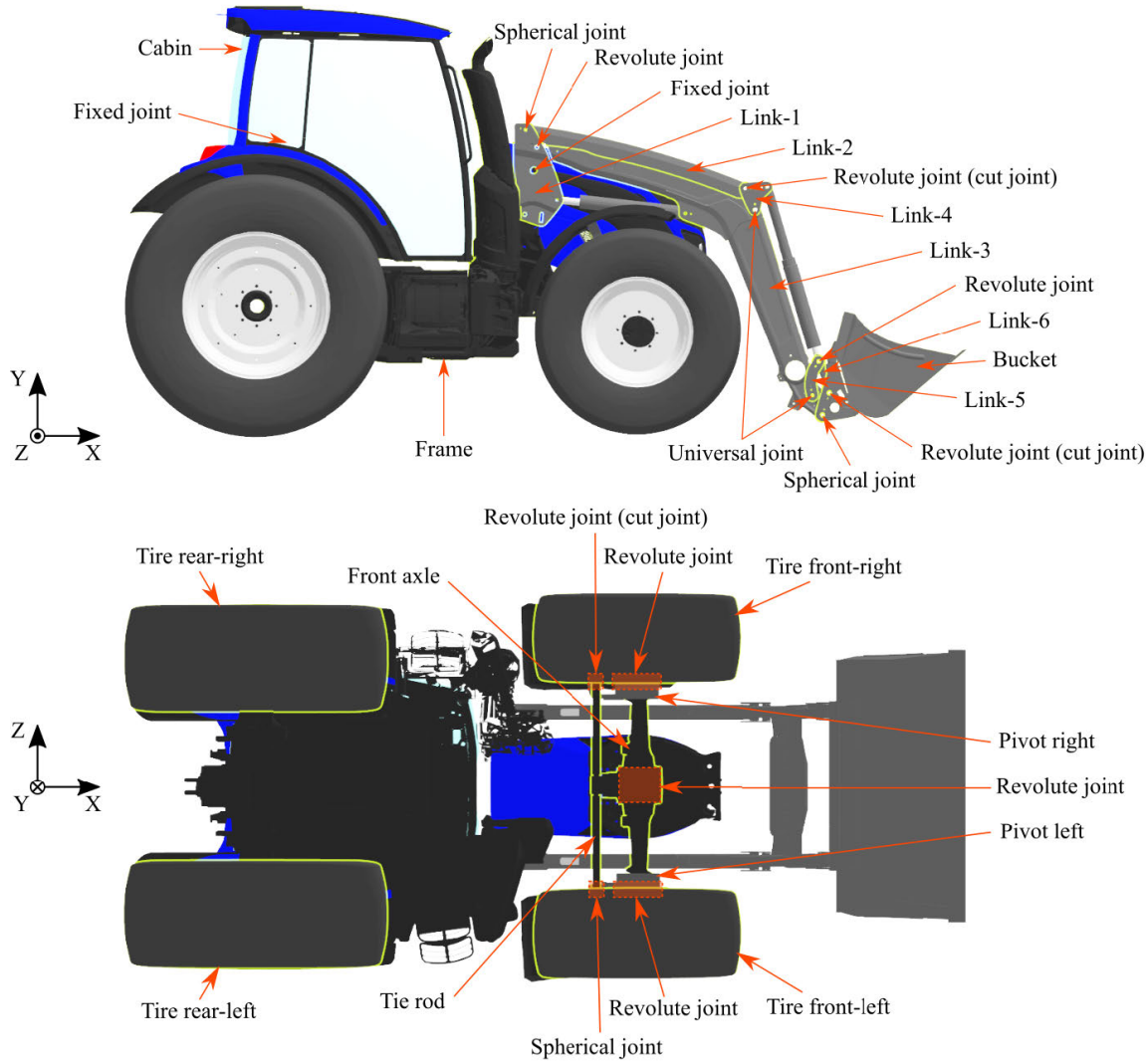

(a) Bodies and joints in the multibody model of the tractor.

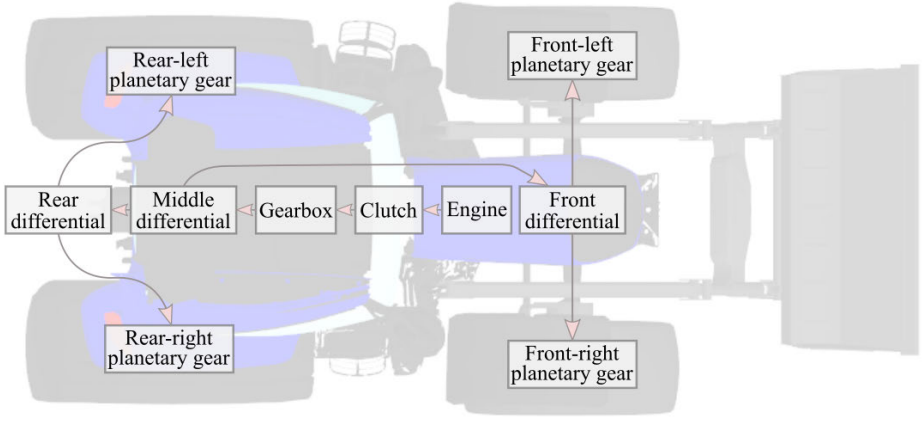

(b) Power transmission system of the tractor.

FIGURE 5. Tractor model used in this study.

for example, in picking an appropriate amount of sand. In general, the designs on a HUD are dependent on a number of factors, especially, from the field of cognitive science, such as symbology, clutter, and viewing comfort issues [60], [65].

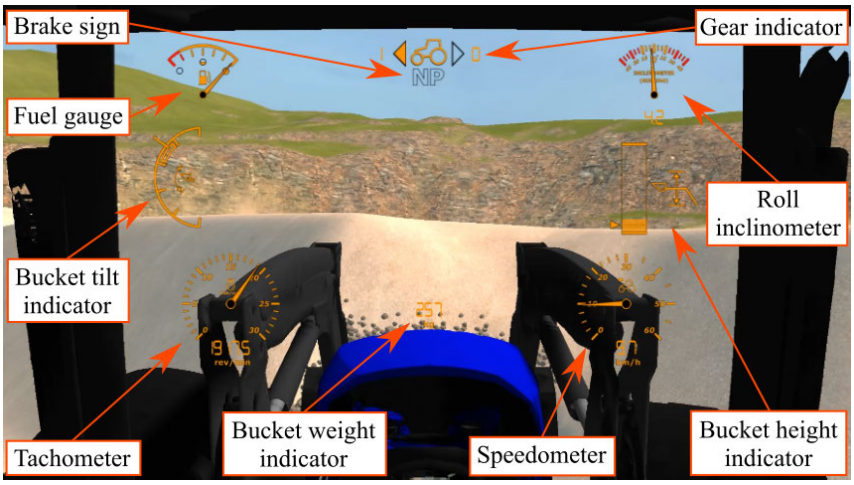

FIGURE 6. Heads-up display unit installed onto the windshield of the tractor [64].

TABLE 1. The elements of the HUD unit used in this study.

Element	Analog gauge	Digital gauge
Tachometer	✓	✓
Speedometer	✓	✓
Roll inclinometer	✓	✓
Gear indicator	✓	✓
Fuel gauge	✓	-
Bucket height indicator	✓	-
Bucket tilt indicator	✓	-
Bucket weight indicator	-	✓

However, this work is only focusing on technical aspects. Here, only one HUD unit is presented onto the windshield to demonstrate the utilization of virtual machine data, which is based on detailed physics-based models, and to assist in task completion. The elements of the HUD unit used in this study are shown in Table 1.

The design of a HUD unit is defined as a scenario, which consists of a series of tasks. Each task is associated with a set of conditions and instructions. The conditions are defined based on value boundaries and the instructions define the gauges and HUD images. These value conditions determine the display of analog and/or digital gauges. The gauges, in turn, describe the gauge type, where for analog gauges, it defines the size and position of the gauge on the windshield of the tractor; and for digital gauges, it defines the size, position, and color of the data on the windshield. Note that the gauges are linked with the data sources of the tractor model, which is defining all the required parameters. Thus, the HUD unit can present the virtual machine data during a real-time simulation. Furthermore, the value conditions can also determine the display of other HUD images, such as an out-of-fuel message, a rollover message, and gear and brake signs.

The data sources of the tractor model, which are linked with the gauges of the HUD unit, are described using virtual sensors installed at a number of locations on the tractor. Note that the virtual sensors are selected in such a way that similar physical sensors could be installed on the real tractor. The tachometer uses the engine speed and the speedometer utilizes the angular velocity and radius of the tires. The data source of the roll inclinometer is described by installing an inclinometer on the cabin of the tractor. An inclinometer is a directional accelerometer that measures the angle of the cabin with respect to the gravity force. The gear indicator utilizes the gear number of the gearbox. The fuel indicator is defined by using the fuel consumption parameter of the engine. The data source associated to the bucket height indicator is described by installing a distance sensor between a point on the front axle and a point on the bucket. The bucket tilt indicator uses data from a rotary encoder installed on the bucket. The data source of the bucket weight indicator is defined by installing a mass sensor near the teeth and inside the bucket. The mass is calculated based on the number of sand particles crossing the mass sensor at the specific location.

It should be noted that the HUD unit offers a gamified experience of the tractor model as shown in Fig. 6. Here, game logics are used to make the HUD unit more interactive during a training. For example, to achieve the goal of moving a certain amount of sand from one place to another, a number of challenges are introduced, such as limited fuel and a limited rolling angle. The HUD unit indicates the critical conditions of the fuel and roll angle by highlighting them in red in the respective analog gauges. If the tractor is out-of-fuel or a rollover has occurred, then the HUD unit shows a breakdown message and the simulation is forced to terminate. Note that a real-time simulator with a two DOFs motion platform is used to provide a realistic experience of the tractor maneuver.

As this study is concerned with the development of tool sets to model HUD units, therefore, only a quantitative evaluation procedure has been employed in this study. Simulation tests are performed by only an inexperienced tractor driver (first author). Before the simulation tests, the participant is given

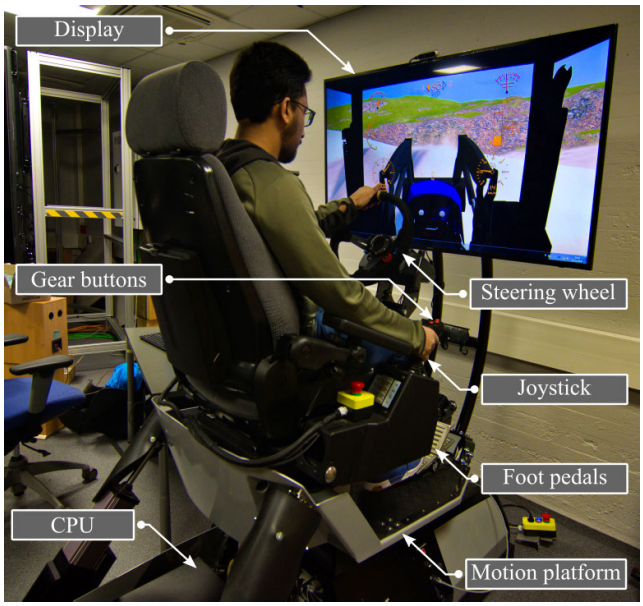

FIGURE 7. Tractor simulator installed with the heads-up display unit.

an opportunity to use the simulator to familiarize himself about the simulation environment and simulator controls. As mentioned above, the goal is to pick a certain amount of sand from a sand pile and dumped onto another place on the ground. The quantitative evaluation is carried out by measuring the amount of sand moved and the movement of the front-loader, such as lifting and tilting of the bucket. The respective gauges are made available to the driver through the HUD unit, where the recommended values of the height and tilt angle of the bucket are marked to collect the maximum amount of sand. These values are provided based on a predetermined evaluation of the sand pile and bucket geometry.

A total of 10 simulations are run to test the utility of the HUD unit and achieve the goal of moving sand, where the driver moved sand ranging from 100 kg to 600 kg, approximately. However, due to a similarity in the results, data for only four simulation tests are presented such that the amount of sand collected in the bucket are approximately 100 kg, 200 kg, 450 kg, and 600 kg. Please note that for conciseness, this paper is focused on demonstrating the utility of the HUD unit that is built using the multibody model of a tractor.

IV. TESTS AND RESULTS

This section presents the simulation results of the real-time multibody model-based HUD unit of a tractor. To test the HUD unit, the simulator setup used is shown in Fig. 7. The used tractor simulator is installed with two degrees of freedom hydraulically driven motion platform to provide a realistic experience of the tractor maneuver. Inputs provided by the driver through the steering wheel, joystick (bucket lifting and tilting), gear buttons (gear index), and foot pedals (accelerate, brake, and clutch) are fed to the central processing unit (CPU). The CPU, in turn, provides output for the display and motion platform. Additionally, the sounds of the engine and movement of the bucket are also provided as an output for a realistic experience. It should be noted that the motion signal provided to the motion platform depends on the undulating terrain of the model and the interaction of the tractor with its surroundings.

A HUD unit incorporated simulator platform can facilitate a training process. Out of a number of simulations performed, data for only four tests are shown in this section for demonstration purpose. The amount of sand collected, and the real-time ability of the system are demonstrated. Additionally, critical conditions such as limited fuel and a limited rolling angle are simulated.

A. PERFORMANCE OF THE HUD UNIT

To achieve the goal of moving a certain amount of sand from one place to another, the tractor model in all four simulation tests follow a three-dimensional maneuver. Figure 8 shows the simulation frames of the HUD unit at different instants of time for the fourth test. By following the HUD unit at 8.50 s, the height and tilt angle of the bucket are adjusted to the recommended values in the bucket height and tilt indicator gauges. The recommended values are marked on the analog gauges to collect a maximum amount of sand in the bucket. The values are predetermined based on the simulation environment, that is, the sand pile. At 10.60 s, the digging operation is performed on a pile of sand that is on the right side in the first and second simulation frames of Fig. 8. After the digging operation at 12.41 s, the bucket is lifted upward and tilted inward as visible in the simulation frame at 14.45 s. During reversing at 17.42 s, the tilt angle of the bucket is slightly adjusted, which is visible in the simulation frame at 26.08 s. At 39.29 s, the sand particles are dumped onto another place of the ground. The tractor maneuver for the fourth test is shown in Fig. 9.

The work cycle shown above demonstrates the utility of the HUD unit in performing a certain task. It provides data such as the weight, height, and tilt of the bucket, thus, it illustrates a quantitative picture of the surroundings of the vehicle. Moreover, the multibody modeling approach provides a physics-based description of the tractor model. Therefore, this multibody-based HUD model can be used in user training and in testing HUDs for various other vehicles.

B. AMOUNT OF SAND COLLECTION

For the simulation tests, the mass of sand particles inside the bucket is shown in Fig. 10a, and the tilt angle and height of the bucket are shown in Fig. 10b. In the process, the bucket is filled with approximately 450 kg, 100 kg, 200 kg, and 600 kg of sand in the consecutive tests, respectively. Otherwise, before the digging and after the dumping operations, the bucket is empty. In all the simulations, the mass inside the bucket fluctuates because of the vibration of the bucket caused either by the tractor reversing or by the hydraulic actuators. During reversing, the tests are performed carefully so that sand particles are not dropped from the bucket.

FIGURE 8. Simulation frames of the HUD unit of the tractor model at different instants of time for the fourth test.

As shown in Fig. 10b, the height and tilt angle of the bucket in every test is adjusted to the recommended value before the digging operation at around 10–11 s. However, varying lifting and tilting of the bucket after the digging process result in different amounts of sand in the bucket. Furthermore, the amount of sand moved is measured for a quantitative evaluation and it can be seen from Fig. 10a that the performance of the driver can be improved with every turn. Therefore, perhaps the HUD unit can help to get accustomed to controls and perform better.

C. REAL-TIME ABILITY OF THE SYSTEM

In this study, a complex multibody model of a tractor is demonstrated, which includes descriptions of hydraulic actuators, contact modeling, tire modeling, and deformable sand field. For all the simulation tests, the loop integration time of the system is shown in Fig. 11. In Fig. 11, the integration time in each time-step is always less than the simulation time-step (1.3 ms) indicating that the simulation step is solved before moving onto the next time-step. Thus, the results demonstrate a computationally efficient system which is real-time enabled. In order words, the real-time capability implies that an output can be received via the display and motion platform as soon as inputs are provided through the steering wheel, joystick, gear buttons, and foot pedals. Therefore, such real-time enabled system can be used in training and other product processes. Furthermore, it should be noted that the loop integration time is low when sand particles are not present, otherwise, the integration time is relatively higher. All the simulations are performed in a C++ environment

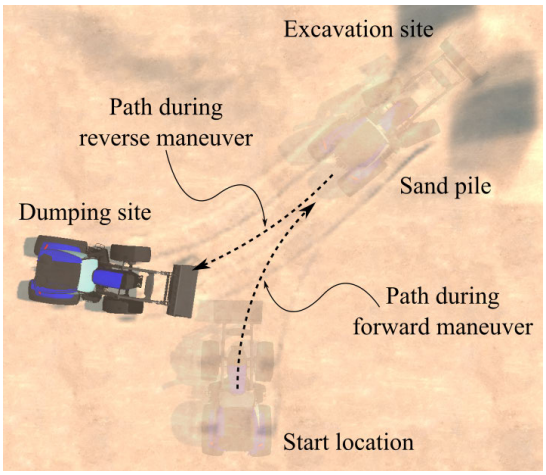

FIGURE 9. Tractor maneuver for the fourth test.

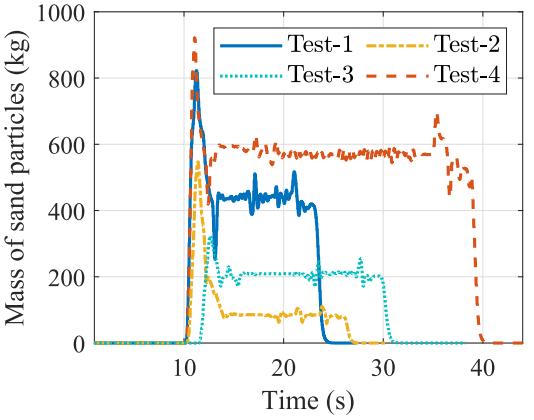

(a) Mass of sand particles in the bucket.

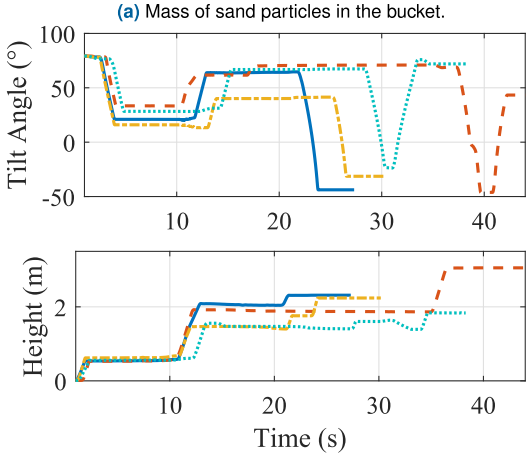

(b) Tilt angle and height of the bucket.

FIGURE 10. Data of bucket weight, tilt, and height indicators of the HUD unit during the simulation tests.

(compiler: Microsoft Visual Studio, version 14.1) and the used hardware/software is shown in Table 2.

In regard to the real-time policy in the C++ environment, the developed simulation application utilizes a *QueryPerformanceCounter* function from Microsoft libraries in the timing function under a *profileapi.h* header. This function retrieves the current value of the performance counter with

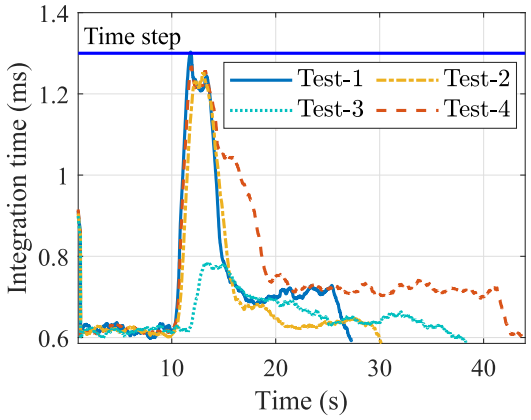

FIGURE 11. Loop integration time of the simulations.

TABLE 2. A description of the used hardware/software.

Name	System used
Operating system	Windows 10
Processor	Intel Core i7 3.41 GHz
Random access memory	64.0 GB
Graphics memory	36809 MB
Display adapter	Nvidia Quadro M2000

a high resolution of 1 µs that is used for the measurement of time-interval. On systems with a Windows XP or later operating systems, this function always succeeds and returns a nonzero value. However, it should be noted that this function is not limited for the loop integration time to reach a predefined simulation time-step at the end of a simulation step. This implies that the loop duration can exceed the real-time requirement and is left to a model designer to define a model simple enough for achieving a real-time simulation.

D. SIMULATING CRITICAL CONDITIONS

The critical conditions of limited fuel and a limited rolling angle are simulated to test the robustness of the HUD unit. Figure 12 shows the simulation frames of the HUD unit when the system is on the verge of meeting the critical conditions. Once the critical condition is met, the HUD unit displays a breakdown message and the simulation is forced to terminate. The limiting criterion for the fuel gauge is 1% of the maximum fuel and for the roll inclinometer, it is 20°.

E. DISCUSSION

The utility of the HUD unit in performing a certain task is demonstrated in Sect. IV-A. It can help to get accustomed to controls and perform better as shown in Sect. IV-B. Furthermore, the real-time capability (Sect. IV-C) and the physics-based modeling of the tractor provided a realistic experience of the tractor. Therefore, it is safe to conclude that the multibody-based HUD model introduced in this study can be used in user training, research, and testing HUDs for various vehicles.

(a) Roll inclinometer reads the maximum permissible roll angle of 20°.

(b) Fuel gauge indicates that the tractor will soon be out-of-fuel.

FIGURE 12. Simulation frames of the HUD unit while simulating critical conditions.

In conclusion, the research questions raised at the beginning of this research has been answered as follows: (a) A HUD can be modeled from a detailed multibody model of a vehicle using virtual sensing; (b) The HUD unit can assist drivers to perform certain tasks by providing a quantitative picture of the surroundings of the vehicle; (c) The proposed HUD modeling approach is robust because it can simulate critical conditions in real-time and is modular because it utilized a multibody modeling approach, thus, contributing to the state-of-the-art.

V. CONCLUSION

This study demonstrated a detailed real-time multibody model-based heads-up display unit of a tractor. The tractor was described using a semi-recursive multibody formulation and the hydraulic actuators were described using the lumped fluid theory. A HUD unit was designed based on a series of tasks that were associated with sets of conditions and instructions. These conditions and instructions determined/designed the analog and digital gauges that were linked with the virtual sensors of the tractor model. The virtual sensors were built using the multibody model of the tractor. The elements of the HUD unit were tachometer, speedometer, roll inclinometer, gear indicator, fuel gauge, and bucket height, tilt, and weight indicators.

The utility of the HUD unit was demonstrated based on a goal of moving a certain amount of sand from one place to another. In all the simulation tests, the tractor model followed a three-dimensional maneuver. The simulation frames of the HUD unit demonstrated its use in assisting a driver to meet the above-mentioned goal. The real-time capability of the system was shown where the loop integration time was always less than the simulation time-step. Such a HUD unit enabled real-time tractor simulator can facilitate a training process. Furthermore, critical conditions such as limited fuel and a limited rolling angle of the tractor were also presented. In conclusion, this study answered all the research questions raised at the beginning of this research and is contributing to the state-of-the-art.

In future work, the proposed method can be used to design HUD units for other complex mobile machines. Various goals can be set to study which goal requires more interaction with the HUD unit. In different operating situations, it can be studied that how a HUD unit contributes to a driver's workload, driving performance, and situational awareness. Moreover, a qualitative evaluation procedure can be carried out to provide more conclusive results about the efficiency and usability of the HUD model through user evaluations. Furthermore, user-centric HUD elements may facilitate a training process and product development. A HUD unit can be installed on an actual tractor and can be implemented for field testing.

REFERENCES

[1] M. Weihrauch, G. Meloeny, and T. Goesch, "The first head-up display introduced by general motors," SAE Tech. Paper 890288, 1989.

[2] J. Akyeampong, S. Udoka, G. Caruso, and M. Bordegoni, "Evaluation of hydraulic excavator human–machine interface concepts using NASA TLX," *Int. J. Ind. Ergonom.*, vol. 44, no. 3, pp. 374–382, May 2014.

[3] A. Pauzie, "Head-up display in automotive: A new reality for the driver," in *Proc. 4th Int. Conf. Design, User Exper., Usability*, Los Angeles, CA, USA, 2015, pp. 505–516.

[4] T. Deng, W. Sun, R. Zhang, and Y. Zhang, "Research on interface design of full windshield head-up display based on user experience," in *Proc. 9th Int. Conf. Appl. Hum. Factors Ergonom.*, Orlando, FL, USA, 2018, pp. 166–173.

[5] D. Beck and W. Park, "Perceived importance of automotive HUD information items: A study with experienced HUD users," *IEEE Access*, vol. 6, pp. 21901–21909, 2018.

[6] Z. An, X. Xu, J. Yang, Y. Liu, and Y. Yan, "A real-time three-dimensional tracking and registration method in the AR-HUD system," *IEEE Access*, vol. 6, pp. 43749–43757, 2018.

[7] J. Ma, Z. Gong, J. Tan, Q. Zhang, and Y. Zuo, "Assessing the driving distraction effect of vehicle HMI displays using data mining techniques," *Transp. Res. F, Traffic Psychol. Behav.*, vol. 69, pp. 235–250, Feb. 2020.

[8] S. Wang, V. Charissis, R. Lagoo, J. Campbell, and D. K. Harrison, "Reducing driver distraction by utilizing augmented reality head-up display system for rear passengers," in *Proc. IEEE Int. Conf. Consum. Electron. (ICCE)*, Las Vegas, NV, USA, Jan. 2019, pp. 1–6.

[9] A. Doshi, S. Y. Cheng, and M. M. Trivedi, "A novel active heads-up display for driver assistance," *IEEE Trans. Syst. Man, Cybern. B, Cybern.*, vol. 39, no. 1, pp. 85–93, Feb. 2009.

[10] Y.-C. Liu and M.-H. Wen, "Comparison of head-up display (HUD) vs. head-down display (HDD): Driving performance of commercial vehicle operators in Taiwan," *Int. J. Hum.-Comput. Stud.*, vol. 61, no. 5, pp. 679–697, Nov. 2004.

[11] D. R. Tufano, "Automotive HUDs: The overlooked safety issues," *Hum. Factors, J. Hum. Factors Ergonom. Soc.*, vol. 39, no. 2, pp. 303–311, Jun. 1997.

[12] A. Gregoriades and A. Sutcliffe, "Simulation-based evaluation of an in-vehicle smart situation awareness enhancement system," *Ergonomics*, vol. 61, no. 7, pp. 947–965, Jul. 2018.
[13] Y.-C. Liu, "Effects of using head-up display in automobile context on attention demand and driving performance," *Displays*, vol. 24, nos. 4–5, pp. 157–165, Dec. 2003.
[14] V. Charissis and S. Papanastasiou, "Human–machine collaboration through vehicle head up display interface," *Cognition, Technol. Work*, vol. 12, no. 1, pp. 41–50, Mar. 2010.
[15] R. Häuslschmid, "Extending head-up displays: Exploring the potential of large and 3D automotive windshield displays," Ph.D. dissertation, Ludwig Maximilian Univ. Munich, Munich, Germany, 2018.
[16] Y. Wu, M. Abdel-Aty, J. Park, and J. Zhu, "Effects of crash warning systems on rear-end crash avoidance behavior under fog conditions," *Transp. Res. C, Emerg. Technol.*, vol. 95, pp. 481–492, Oct. 2018.
[17] S. Wang, Y. Wang, Q. Zheng, and Z. Li, "Guidance-oriented advanced curve speed warning system in a connected vehicle environment," *Accident Anal. Prevention*, vol. 148, pp. 105801-1–105801-24, Dec. 2020.
[18] G. J. Heydinger, M. K. Salaani, W. R. Garrott, and P. A. Grygier, "Vehicle dynamics modelling for the national advanced driving simulator," *Proc. Inst. Mech. Eng., D, J. Automobile Eng.*, vol. 216, no. 4, pp. 307–318, Apr. 2002.
[19] R. Lagoo, V. Charissis, W. Chan, S. Khan, and D. Harrison, "Prototype gesture recognition interface for vehicular head-up display system," in *Proc. IEEE Int. Conf. Consum. Electron. (ICCE)*, Las Vegas, NV, USA, Jan. 2018, pp. 1–6.
[20] H. Wu, Y. Wang, J. Liu, J. Qiu, and X. Zhang, "User-defined gesture interaction for in-vehicle information systems," *Multimedia Tools Appl.*, vol. 79, nos. 1–2, pp. 263–288, Jan. 2020.
[21] R. Lagoo, V. Charissis, and D. K. Harrison, "Mitigating driver's distraction: Automotive head-up display and gesture recognition system," *IEEE Consum. Electron. Mag.*, vol. 8, no. 5, pp. 79–85, Sep. 2019.
[22] V. Charissis, J. Falah, R. Lagoo, S. F. M. Alfalah, S. Khan, S. Wang, S. Altarteer, K. B. Larbi, and D. Drikakis, "Employing emerging technologies to develop and evaluate in-vehicle intelligent systems for driver support: Infotainment AR HUD case study," *Appl. Sci.*, vol. 11, no. 4, p. 1397, Feb. 2021.
[23] Z. Wang, X. Liao, C. Wang, D. Oswald, G. Wu, K. Boriboonsomsin, M. J. Barth, K. Han, B. Kim, and P. Tiwari, "Driver behavior modeling using game engine and real vehicle: A learning-based approach," *IEEE Trans. Intell. Vehicles*, vol. 5, no. 4, pp. 738–749, Dec. 2020.
[24] C. Merenda, C. Suga, J. L. Gabbard, and T. Misu, "Effects of real-world visual fidelity on AR interface assessment: A case study using AR head-up display graphics in driving," in *Proc. 19th Int. Symp. Mixed Augmented Reality*, Beijing, China, 2019, pp. 145–156.
[25] S. Kim and A. K. Dey, "Simulated augmented reality windshield display as a cognitive mapping aid for elder driver navigation," in *Proc. 27th Int. Conf. Hum. Factors Comput. Syst. (CHI)*, Boston, MA, USA, 2009, pp. 133–142.
[26] C. Merenda, H. Kim, K. Tanous, J. L. Gabbard, B. Feichtl, T. Misu, and C. Suga, "Augmented reality interface design approaches for goal-directed and stimulus-driven driving tasks," *IEEE Trans. Vis. Comput. Graphics*, vol. 24, no. 11, pp. 2875–2885, Nov. 2018.
[27] M.-K. Choi, J.-H. Lee, H. Jung, I. R. Tayibnapis, and S. Kown, "Simulation framework for improved UI/UX of AR-HUD display," in *Proc. IEEE Int. Conf. Consum. Electron. (ICCE)*, Las Vegas, NV, USA, Jan. 2018, pp. 1–4.
[28] T. Hasegawa, Y. Sumiyosi, Y. Hayashi, A. Nishikawa, T. Chikuri, and O. Tsukahara, "Position correction against vehicle vibration for augmented reality on head-up display," in *SID Symp. Dig. Tech. Papers*, San Jose, CA, USA, 2019, pp. 1404–1407.
[29] M. Blundell and D. Harty, *The Multibody Systems Approach to Vehicle Dynamics*. Oxford, U.K.: Butterworth-Heinemann, 2015.
[30] J. G. De Jalon and E. Bayo, *Kinematic and Dynamic Simulation of Multibody Systems: The Real-Time Challenge*. New York, NY, USA: Springer-Verlag, 1994.
[31] Z. Zou, X. Pang, and J. Chen, "Comprehensive theoretical digging performance analysis for hydraulic excavator using convex polytope method," *Multibody Syst. Dyn.*, vol. 47, no. 2, pp. 137–164, Oct. 2019.
[32] S. Jaiswal, M. I. Islam, L. Hannola, J. Sopanen, and A. Mikkola, "Gamification procedure based on real-time multibody simulation," *Int. Rev. Model. Simul.*, vol. 11, no. 5, pp. 259–266, 2018.
[33] D. Dopico, A. Luaces, M. Gonzalez, and J. Cuadrado, "Dealing with multiple contacts in a human-in-the-loop application," *Multibody Syst. Dyn.*, vol. 25, no. 2, pp. 167–183, Feb. 2011.
[34] A. Nicolini, F. Mocera, and A. Somà, "Multibody simulation of a tracked vehicle with deformable ground contact model," *Proc. Inst. Mech. Eng., K, J. Multi-Body Dyn.*, vol. 233, no. 1, pp. 152–162, Mar. 2019.
[35] M. E. Baharudin, A. Rouvinen, P. Korkealaakso, and A. Mikkola, "Real-time multibody application for tree harvester truck simulator," *Proc. Inst. Mech. Eng., K, J. Multi-Body Dyn.*, vol. 228, no. 2, pp. 182–198, Jun. 2014.
[36] S. Jaiswal, P. Korkealaakso, R. Åman, J. Sopanen, and A. Mikkola, "Deformable terrain model for the real-time multibody simulation of a tractor with a hydraulically driven front-loader," *IEEE Access*, vol. 7, pp. 172694–172708, 2019.
[37] J. Torres-Moreno, J. Blanco-Claraco, A. Giménez-Fernández, E. Sanjurjo, and M. Naya, "Online kinematic and dynamic-state estimation for constrained multibody systems based on IMUs," *Sensors*, vol. 16, no. 3, p. 333, Mar. 2016.
[38] E. Sanjurjo, D. Dopico, A. Luaces, and M. Á. Naya, "State and force observers based on multibody models and the indirect Kalman filter," *Mech. Syst. Signal Process.*, vol. 106, pp. 210–228, Jun. 2018.
[39] A. Avello, J. M. Jiménez, E. Bayo, and J. G. de Jalón, "A simple and highly parallelizable method for real-time dynamic simulation based on velocity transformations," *Comput. Methods Appl. Mech. Eng.*, vol. 107, no. 3, pp. 313–339, Aug. 1993.
[40] J. Watton, *Fluid Power Systems: Modeling, Simulation, Analog and Microcomputer Control*. Cambridge, U.K.: Prentice-Hall, 1989.
[41] S. Gottschalk, M. C. Lin, and D. Manocha, "OBBtree: A hierarchical structure for rapid interference detection," in *Proc. 23rd Annu. Conf. Comput. Graph. Interact. Techn.*, New Orleans, LA, USA, 1996, pp. 171–180.
[42] E. Drumwright, "A fast and stable penalty method for rigid body simulation," *IEEE Trans. Vis. Comput. Graphics*, vol. 14, no. 1, pp. 231–240, Jan. 2008.
[43] C. C. D. Wit, R. Horowitz, and P. Tsiotras, *New Directions in Nonlinear Observer Design*. London, U.K.: Springer, 1999.
[44] C. C. D. Wit and P. Tsiotras, "Dynamic tire friction models for vehicle traction control," in *Proc. 38th IEEE Conf. Decis. Control*, Phoenix, AZ, USA, Dec. 1999, pp. 3746–3751.
[45] E. Bayo, J. G. De Jalon, and M. A. Serna, "A modified Lagrangian formulation for the dynamic analysis of constrained mechanical systems," *Comput. Methods Appl. Mech. Eng.*, vol. 71, no. 2, pp. 183–195, Nov. 1988.
[46] H. M. Handroos and M. J. Vilenius, "Flexible semi-empirical models for hydraulic flow control valves," *J. Mech. Des.*, vol. 113, no. 3, pp. 232–238, Sep. 1991.
[47] S. Jaiswal, E. Sanjurjo, J. Cuadrado, J. Sopanen, and A. Mikkola, "State estimator based on an indirect Kalman filter for a hydraulically actuated multibody system," *Multibody Syst. Dyn.*, pp. 1–25, Dec. 2020.
[48] S. Jaiswal, J. Sopanen, and A. Mikkola, "Efficiency comparison of various friction models of a hydraulic cylinder in the framework of multibody system dynamics," *Nonlinear Dyn.*, pp. 1–17, Apr. 2021.
[49] M. Moore and J. Wilhelms, "Collision detection and response for computer animation," in *Proc. 15th Annu. Conf. Comput. Graph. Interact. Techn.*, Atlanta, GA, USA, 1988, pp. 289–298.
[50] P. R. Dahl, "A solid friction model," Aerosp. Corp., El Segundo, CA, USA, Tech. Rep. TOR-0158(3107-18)-1, 1968.
[51] J. Cuadrado, D. Dopico, M. A. Naya, and M. Gonzalez, "Penalty, semi-recursive and hybrid methods for MBS real-time dynamics in the context of structural integrators," *Multibody Syst. Dyn.*, vol. 12, no. 2, pp. 117–132, Sep. 2004.
[52] J. Cuadrado, D. Dopico, M. Gonzalez, and M. A. Naya, "A combined penalty and recursive real-time formulation for multibody dynamics," *J. Mech. Des.*, vol. 126, no. 4, pp. 602–608, Jul. 2004.
[53] Y. Pan, S. Xiang, Y. He, J. Zhao, and A. Mikkola, "The validation of a semi-recursive vehicle dynamics model for a real-time simulation," *Mechanism Mach. Theory*, vol. 151, Sep. 2020, Art. no. 103907.
[54] Y. Pan, S. Xiang, and A. Mikkola, "An efficient high-order time-step algorithm with proportional-integral control strategy for semirecursive vehicle dynamics," *IEEE Access*, vol. 7, pp. 40833–40842, 2019.
[55] Y. Pan, W. Dai, L. Huang, Z. Li, and A. Mikkola, "Iterative refinement algorithm for efficient velocities and accelerations solutions in closed-loop multibody dynamics," *Mech. Syst. Signal Process.*, vol. 152, May 2021, Art. no. 107463.
[56] S. Jaiswal, J. Rahikainen, Q. Khadim, J. Sopanen, and A. Mikkola, "Comparing double-step and penalty-based semirecursive formulations for hydraulically actuated multibody systems in a monolithic approach," *Multibody Syst. Dyn.*, pp. 1–23, Jan. 2021, doi: 10.1007/s11044-020-09776-4.

[57] L. Morra, F. Lamberti, F. G. Pratticó, S. L. Rosa, and P. Montuschi, "Building trust in autonomous vehicles: Role of virtual reality driving simulators in HMI design," *IEEE Trans. Veh. Technol.*, vol. 68, no. 10, pp. 9438–9450, Oct. 2019.
[58] R. Li, Y. V. Chen, L. Zhang, Z. Shen, and Z. C. Qian, "Effects of perception of head-up display on the driving safety of experienced and inexperienced drivers," *Displays*, vol. 64, pp. 101962-1–101962-10, Sep. 2020.
[59] R. Häuslschmid, S. Osterwald, M. Lang, and A. Butz, "Augmenting the driver's view with peripheral information on a windshield display," in *Proc. 20th Int. Conf. Intell. User Interfaces*, Atlanta, GA, USA, Mar. 2015, pp. 311–321.
[60] N. J. Ward and A. Parkes, "Head-up displays and their automotive application: An overview of human factors issues affecting safety," *Accident Anal. Prevention*, vol. 26, no. 6, pp. 703–717, Dec. 1994.
[61] R. J. Sojourner and J. F. Antin, "The effects of a simulated head-up display speedometer on perceptual task performance," *Hum. Factors, J. Hum. Factors Ergonom. Soc.*, vol. 32, no. 3, pp. 329–339, Jun. 1990.
[62] K. G. Tippey, E. Sivaraj, and T. K. Ferris, "Driving while interacting with Google glass: Investigating the combined effect of head-up display and hands-free input on driving safety and multitask performance," *Hum. Factors, J. Hum. Factors Ergonom. Soc.*, vol. 59, no. 4, pp. 671–688, Jun. 2017.
[63] W. Yiwei, Y. Xianghai, and Z. Zhili, "Architecture modeling and test of tractor power shift transmission," *IEEE Access*, vol. 9, pp. 3517–3525, 2021.
[64] S. Jaiswal, A. Tarkiainen, T. Choudhury, J. Sopanen, and A. Mikkola, "Gamification and the marketing of agricultural machinery," in *Real-Time Simulation for Sustainable Production: Enhancing User Experience and Creating Business Value*. Evanston, IL, USA: Routledge, Jan. 2021.
[65] J. H. Iavecchia, H. P. Iavecchia, and I. S. N. Roscoe, "Eye accommodation to head-up virtual images," *Hum. Factors, J. Hum. Factors Ergonom. Soc.*, vol. 30, no. 6, pp. 689–702, Dec. 1988.

SURAJ JAISWAL was born in Kolkata, India, in July 1991. He received the B.E. degree in production engineering from Jadavpur University, Kolkata, in 2013, and the M.S. degree in mechanical engineering from the Lappeenranta University of Technology, Lappeenranta, Finland, in 2017, where he is currently pursuing the Ph.D. degree in mechanical engineering.

From 2013 to 2015, he has worked as a Design Engineer with Tata Consultancy Services Ltd., Kolkata. Since 2016, he has been working as a Junior Research Assistant with the Lappeenranta University of Technology. His research interests include multibody dynamics, non-linear Kalman filters, real-time simulation, and vehicle dynamics.

Mr. Jaiswal received the "Best Paper Award" at the 9th Asian Conference on Multibody Dynamics (ACMD 2018) held in Xian, China, during August 19–23, 2018.

RAFAEL ÅMAN was born in Karkkila, Finland, in 1978. He received the B.S. degree in mechanical engineering from the Helsinki University of Applied Sciences (Stadia), Finland, in 2002, and the M.S. and Ph.D. degrees in mechanical engineering from the Lappeenranta University of Technology, Lappeenranta, Finland, in 2007 and 2011, respectively, all in mechatronics.

From 2006 to 2016, he has worked as a Researcher on the simulation of fluid power circuits, hybrid power transmission, and energy recovery systems with the Lappeenranta University of Technology. He also has work experience as a Service Engineer in a civil engineering company. Since 2016, he has been with AGCO Corporation. He works at Valtra Inc., Suolahti, Finland. His main responsibilities have included system simulations and tractor design validation tests, as well as research and advanced engineering. As the Technical Specialist, he focuses on the use of future technologies in agricultural machinery and in their research and development processes. He has contributed to 26 scientific publications and presentations.

JUSSI SOPANEN (Member, IEEE) was born in Enonkoski, Finland, in 1974. He received the M.S. degree in mechanical engineering and the Ph.D. degree (in technology) from the Lappeenranta University of Technology, Lappeenranta, Finland, in 1999 and 2004, respectively.

From 1999 to 2006, he has worked as a Researcher with the Department of Mechanical Engineering, Lappeenranta University of Technology. From 2004 to 2005, he has worked as a Product Development Engineer for the electric machine manufacturer Rotatek Finland Ltd. From 2006 to 2012, he has worked as the Principal Lecturer in mechanical engineering and the Research Manager of the Faculty of Technology, Saimaa University of Applied Sciences, Lappeenranta. He is currently a Professor of machine dynamics with the Lappeenranta University of Technology. His research interests include rotor dynamics, multibody dynamics, and the mechanical design of electrical machines.

AKI MIKKOLA received the Ph.D. degree in the field of machine design in 1997.

Since 2002, he has been working as a Professor with the Department of Mechanical Engineering, Lappeenranta University of Technology, Lappeenranta, Finland. He is currently leading the Research Team of the Laboratory of Machine Design, Lappeenranta University of Technology. His research interests include machine dynamics and vibration, multibody system dynamics, and bio-mechanics. He has been awarded five patents and has contributed to more than 90 peer-reviewed journal articles.